Check for updates

Brookite, a sometimes under evaluated TiO$_2$ polymorph

Maela Manzoli, [ID] [a] Francesca S. Freyria,[b] Nicola Blangetti[b] and Barbara Bonelli [ID] *[b]

Some of the advancements concerning the study of phase-pure brookite and, especially, brookite-containing TiO$_2$ mixed phases are reviewed. Relevance is given to their prospective photocatalytic applications, where the (positive) effect of the presence of brookite has been demonstrated, especially when solar light is concerned. From the literature, it emerges that, besides the band gap determination, which still requires more detailed studies (band gap values in a wide range are reported), the roles of brookite-containing heterojunctions, of the surface properties (*i.e.* acidity, redox behaviour, and the presence of coordinatively unsaturated sites), of the particular crystalline structure and of brookite influence on the anatase to rutile transition are crucial for its applications in the field of (solar) photocatalysis and electrocatalysis, but also electrochemical applications (*i.e.* Li batteries). The need emerges for a deeper understanding of the physico-chemical phenomena underlying their (recently demonstrated) capacity of stabilizing photogenerated electron/hole pairs. In perspective, the development of green synthesis methods to tailor the surface and structural properties of phase-pure brookite and brookite-containing mixed phases could extend their photo- and electrochemical applications.

[a]Dipartimento di Scienza e Tecnologia del Farmaco, NIS – Centre for Nanostructured Interfaces and Surfaces, University of Turin, Via P. Giuria 9, I-10125 Torino, Italy
[b]Dipartimento di Scienza Applicata e Tecnologia and INSTM Unit of Torino – Politecnico, Corso Duca degli Abruzzi 24, I-10129 Torino, Italy. E-mail: barbara. bonelli@polito.it

1. Introduction: why brookite?

TiO$_2$ has several polymorphs: although less-known amorphous TiO$_2$ and monoclinic TiO$_2$–B (space group $C2/m$) are gaining growing interest, anatase (tetragonal crystal system), rutile (tetragonal) and brookite (orthorhombic) are the most studied polymorphs, belonging to the $I4_1/amd$, $P4_2/mnm$ and $Pbca$ space

Maela Manzoli received a PhD in Chemical Science at the University of Torino (Italy) in 2001. Her skills are the study of surface properties of nanostructured catalysts (oxides and supported metal nanoparticles) as well as their textural, morphological and structural characterisation before and after reaction to establish structure–activity relationships. She is currently Associate Professor of Industrial Chemistry at the Department of Drug Science and Technology, University of Torino, where she started the development of new catalytic processes assisted by MW, US or mechanochemistry in batch or flow reactors. She has authored >140 peer-reviewed papers and 3 book chapters (H-index: 42).

After a MEng in Environmental Engineering, Francesca S. Freyria received a European PhD degree in Materials Science and Technology at Politecnico di Torino. In 2014, she joined Professor Bawendi's group at the Department of Chemistry, Massachusetts Institute of Technology (MA, USA) as a Postdoctoral Associate. In 2020, she started her Marie Skłodowska-Curie Actions Individual Fellowship (IF) at the Department of Applied Science and Technology, Politecnico of Torino (Project: LuSH Art-Luminescent Solar Heterostructures for Artificial photosynthesis). Her research interests are the study and synthesis of new heterostructured nanomaterials, to endow them with new properties for solar energy and environmental remediation applications.

groups, respectively. Table 1 summarises the conventional unit cells along with the lattice parameters and volumes of anatase, rutile and brookite polymorphs obtained from Density Functional Theory (DFT) calculations and experiments.[1] The formation of different polymorphs depends on how the TiO_6^{2-} octahedral units share edges and corners: for instance, the TiO_6^{2-} units in anatase, rutile and brookite share four, two and three edges, respectively.[1,2]

The theoretically predicted relative phase stability (rutile > brookite > anatase) agrees with experimental findings: rutile is the most stable phase, whereas anatase, and brookite (and TiO_2–B) are metastable phases and tend to transform into rutile at high temperature (T).[1] Brookite has a more disordered structure than rutile and anatase, in that the six Ti–O bonds in the octahedral units have different lengths:[2] this fact affects its behaviour under pressure, as detailed in the following. Bulk anatase transforms into rutile, the thermodynamically stable phase, at $ca.$ 600 °C in air, whereas for nanometric TiO_2 the reported transition T varies in a broad range (400–1200 °C).[3] Anatase is characterized by the lowest surface energy (as compared to rutile and brookite), and, thus, it is relatively simple to obtain anatase nanoparticles (NPs), which are employed in most photocatalytic studies, notwithstanding its band gap energy (E_g, $ca.$ 3.2 eV, Table 1)[4] is larger than that of rutile ($ca.$ 3.0 eV, Table 1), but the higher density and smaller specific surface area of rutile NPs hamper its photocatalytic applications. The average E_g values of brookite reported by the literature span, instead, in a wide range (3.1–3.4 eV, Table 1).

For photocatalytic applications, the type of electron transition is crucial: there is currently agreement about the fact that the transition is phonon-assisted in anatase, which is an indirect semi-conductor with lower probability of recombination of photogenerated electron/hole (e^-/h^+) than both rutile and brookite, which are currently considered as direct semi-conductors, where the e^-/h^+ recombination is facilitated, finally lowering the quantum efficiency (Fig. 1).[4]

Another reason of the superior photocatalytic activity of anatase is that electrons in anatase have a smaller effective mass, thus they migrate more easily to participate to photocatalytic reactions. This fact affects the photocatalytic performance of anatase, along with smaller NPs size (due to lower surface energy) and longer lifetime of charge carriers (due to the indirect transition).[4]

Interest for brookite is emerging in the last years, as testified by Fig. 2, reporting the growing number of brookite-related papers (blue curve) in the most recent three decades (1990–2022 range, Source: Scopus database), along with the number of published papers if the keywords "photocatalysis" (orange curve) and "photocatalyst" (dark blue curve) are added to the search. Interestingly, the publications in which brookite is in some way connected with photocatalytic applications started to appear only ten years later.

The recent scientific interest into brookite is likely related to the sometimes-difficult synthesis of phase-pure brookite, as transition to more stable phases occurs during the thermal treatments that are the last step of most synthesis procedures.

Currently, several synthesis procedures allow obtaining phase-pure brookite,[5] although for most applications (e.g. photocatalysis) brookite containing mixed phase TiO_2 outperforms phase-pure TiO_2, due to a favourable bands alignment, as detailed in the following.[5,6]

As detailed in Table 1, the density of the three polymorphs decreases in the order rutile > brookite > anatase, with brookite having a kind of "hybrid" nature between rutile and anatase.

This trend is also observed for the refractive index of the three phases (Table 2), as evidenced by Posternak et al.[7] who pointed out the "hybrid nature" of the brookite polymorph. The nature of the crystalline structure and of the brookite surface, in terms of exposed facets, acidic properties and redox behaviour

After obtaining a bachelor's degree in Materials Engineering at Politecnico di Torino (Italy), Nicola Blangetti obtained a Master's degree with a final dissertation on the "Photocatalytic degradation of nitrogen containing pollutants" under the supervision of Barbara Bonelli and Francesca S. Freyria. He, then, continued his academic career by starting a PhD in Material Science and Technology in the research group of Prof. Bonelli (www.scm.polito.it). During his PhD, he has focused on the synthesis and characterization of TiO_2-based materials with the aim of studying, inter alia, the correlation between polymorphic structure heterojunctions and photocatalytic activity under sunlight and UV light.
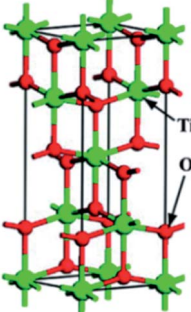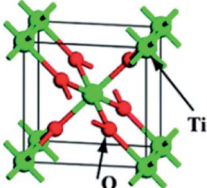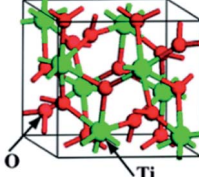
Barbara Bonelli holds a PhD in Chemical Science from the University of Torino (Italy) and a Master's degree in Industrial Chemistry (magna cum laude) from the same Institution. In 2005, she was appointed Assistant Professor at Politecnico di Torino (Italy), where she has been Associate Professor since 2010, and Full Professor of Chemical Fundamentals for Engineering since 2021. She is currently Chair of the PhD program in Materials Science and Technology. Born as a spectroscopist, she extended her research interests to nanoporous materials for gas adsorption/storage, removal of water emerging pollutants, biomolecules detection, catalysis and photocatalysis. She has authored >180 peer-reviewed papers and several book chapters (H-index: 33).

RSC Advances

Review

Table 1 Conventional unit cells along with optimized lattice parameters, volumes (V) and relative deviations, and experimental and calculated average E_g for anatase, rutile and brookite TiO_2. All deviations are less than 3%, which is consistent with the reliability of the DFT calculations performed in ref. 1

Polymorph	Unit cell[a]	Method	a (Å)	b (Å)	c (Å)	V (Å³)	$\alpha = \beta = \gamma$ (°)	Average E_g (eV)	DFT[1] E_g (eV)
		Experimental	3.796	3.796	9.444	136.084	90		
		DFT	3.800	3.800	9.700	140.068	90		
		Deviation (%)	0.1	0.1	2.7	3.0	0		
Anatase								3.2	2.38
		Experimental	4.602	4.602	2.956	62.603	90		
		DFT	4.643	4.643	2.965	63.918	90		
		Deviation (%)	0.9	0.9	0.3	2.1	0		
Rutile								3.0	2.13
		Experimental	9.166	5.436	5.135	255.858	90		
		DFT	9.257	5.501	5.177	263.627	90		
		Deviation (%)	1.0	1.2	0.8	3.0	0		
Brookite								3.1–3.4	1.86

[a] Adapted from ref. 4 with permission from the Royal Society of Chemistry.

are extremely interesting issues. Concerning the surface reactivity, indeed, some facets are more reactive than others and this may affect, in turn, the final catalytic and photocatalytic activity.[9] The type and abundance of Ti^{4+} sites on the different exposed crystalline facets and of Ti^{3+} sites, forming by Ti^{4+} reduction and giving rise to self-doping, as well as the ability to withstand oxygen vacancies, can be responsible of a peculiar behaviour of the brookite surface, in particular its higher (Lewis) acidity and ability to stabilize Ti^{3+} species.[10] Another point of interest is the ability of the brookite structure to host foreign ions, like Li^+ ions, which could be potentially useful for electrochemical applications.[8]

2. About the synthesis of brookite

2.1. Traditional methods to obtain phase-pure brookite and brookite-containing mixed phase TiO_2

The synthesis of TiO_2 NPs in liquid phase implies the hydrolysis of Ti salts/alkoxides to obtain $TiO^{2+}/Ti(OH)_2^{2+}$ species that undergo olation/oxolation to $(TiO_2)^{n-}$ chains and, then, polymerization into aggregates.

With anatase, several methods allow controlling NPs crystal phase and shape, as well as the exposure of preferred crystalline

planes, whereas[1] the synthesis of phase-pure brookite TiO_2 faced the issue of its metastability, as mentioned in the Introduction. More recently, the number of papers on the synthesis of phase-pure brookite is increasing (Fig. 2).

As a whole, the different methods reported are mostly based on hydrothermal and/or solvothermal treatments consisting in many, time-demanding and energy-consuming steps. Varying some parameters, like type of solvent, acid/base type, pH, presence of a template, presence of a ligand, type of precursor, *etc.* allows tuning the composition of the final phase: phase-pure brookite can be obtained, for instance, by hydrothermal treatment of an amorphous TiO_2 precursor produced, in turn, by sol–gel method.[11]

Besides the need of multi-step procedures, in aqueous environment it is difficult to control brookite crystals growth. For this reason, alternative methods are reported, like a non-aqueous one-pot solvothermal (in ethanol) from tetrabutyltitanate $(Ti(OBu)_4)$ and sodium fluoride (NaF) to produce brookite nanorods.[12] The presence of NaF was essential to promote the growth of (highly phase-pure) brookite nanorods after 24 hours in autoclave at 180 °C, without subsequent calcination, during which the occurrence of Na^+ ions was considered to favour the formation of brookite, whereas the alcoholysis of $Ti(OBu)_4$
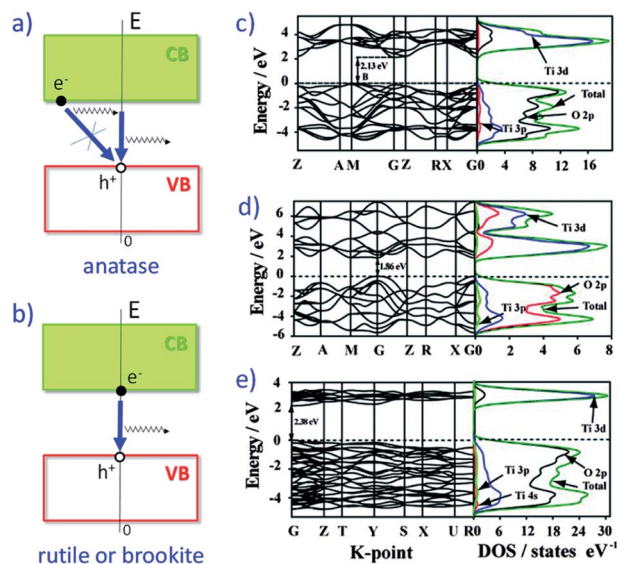
Fig. 1 Indirect band gap of anatase (a) making direct recombination of photogenerated e^- from conduction band (CB) with h^+ from valence band (VB) less probable, thus increasing the e^-/h^+ lifetime relative to direct band gap of rutile or brookite (b). Band structure and density of states for (c) anatase, (d) rutile and (e) brookite. Partially adapted from ref. 4 with permission from the Royal Society of Chemistry.
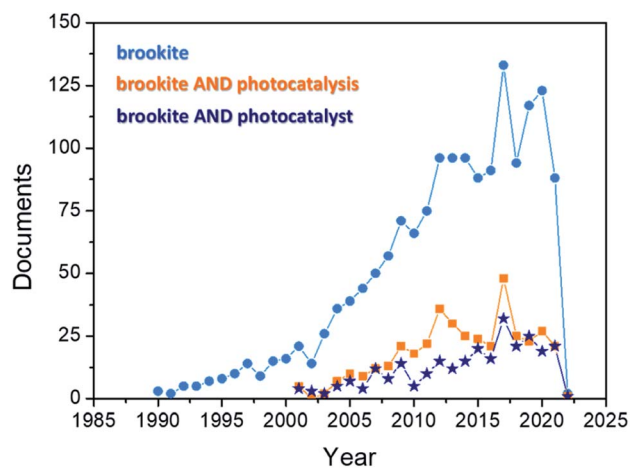

Fig. 2 Number of brookite-related papers from 1990. Source: Scopus database.

that Na^+ ions[12] stabilize the (bi-dimensional) titanate species, forming sheets that preferentially crystallize into brookite, whereas the presence of NH_4^+ ions favours the formation of anatase.[13]

Soft-template (PEG, PolyEthylene Glycol) assisted sol–gel synthesis was adopted to obtain phase-pure brookite and mixed brookite/rutile phases, where PEG led to the formation of inter-particle pores, particularly useful for photocatalytic applications.[14] The specific synthesis conditions (i.e. a concentration of HCl equal to 0.025 M) led to phase-pure brookite stable up to 400 °C (the adopted calcination T), whereas more concentrated HCl solution (0.15 M) led to brookite/rutile mixtures already after calcination at ca. 330 °C, with complete transition to rutile above 600 °C, the higher protons concentration being responsible of promoting the transition to rutile.

The role of HCl in driving the preferential formation of brookite and rutile (as compared to anatase) has been demonstrated also in another work concerning the synthesis of phase-pure TiO_2 NPs by hydrothermal treatment of an amorphous TiO_2 as precursor: anatase NPs were obtained using acetic acid at 200 °C, while phase-pure rutile and brookite NPs were obtained using 4 M HCl at 200 °C and 3 M HCl at 175 °C.[15] According to the authors, the formation of anatase NPs was favoured by the (low) surface energy of this polymorph; the formation of both rutile and brookite, instead, occurs via a dissolution-precipitation mechanism, through which the chains of TiO_6^{2-} units arrange into different crystalline structures, depending on the adopted chemical reagent, giving rise to brookite and rutile. Finally, under hydrothermal conditions, the particles growth kinetics is the result of coarsening and aggregation–recrystallization processes, through which control of the average NPs size is possible.[15]

Alternatively, the presence of ligands allows obtaining (phase-pure) brookite. Several synthesis procedures with different ligands and at different pH values have been reported: the idea is that $[TiL_6]^{z+}$ octahedral charged complexes form in water, in which the nature of the ligand (L) depends on the solution pH and the complexing agent.

Such octahedral complexes can, then, self-assemble in the initial structures of anatase, rutile and brookite crystallites: for instance, Wang et al.[16] showed that oxalic acid is a complexing agent, which can favour the formation of brookite under specific pH conditions with the assistance of NaOH (i.e., not alone) at mildly basic pH values, below 10. The so obtained brookite nanostructures were thermally stable (i.e., no phase transition occurred) up to 700 °C: calcination at 300, 400, 500, 600 and 700 °C only brought about an increase in the crystallite

alone in ethanol resulted in phase-pure anatase NPs.[12] The positive effect of the presence of Na^+ ions on the synthesis of phase-pure brookite has been noticed also by other authors, in

Table 2 Density (g cm^{-3}), diameter of stable NPs (d in nm), calculated depth of electron traps (eV), flat band potential (E_{FB}), Fermi potential (E_F) for anatase, rutile and brookite TiO_2

Polymorph	Density (g cm^{-3})	Diameter (d) of stable NPs (nm)[17,18]	Calculated depth of the electrons trap[51] (eV)	E_{FB}[21] [V vs. NHE]	E_F[21] [V vs. NHE]
Anatase	3.895	$d < 11$	<0.1 (0–0.2 eV)	−0.35	−0.68
Rutile	4.24	$d < 35$	>0.9 (0.8–1 eV)		
Brookite	4.13	$11 < d < 35$	≈0.4 (none)	−0.54	−0.77

size (from 27.65 to 35.93 nm). According to Table 2, stable brookite NPs should have a diameter in the 11–35 nm range, whereas more stable anatase NPs have a size below 14 nm and rutile NPs are more stable when their size is larger than 35 nm.[17,18]

Another method consists in the precipitation of hydrous powders from $TiCl_4$ at varying pH values, as obtained by addition of aqueous ammonia, followed by calcination at 450 °C.[19] The resulting powders consisted into nanocrystalline anatase/brookite mixed phases where the volume fraction of the brookite phase increased at lower pH values.

Highly crystalline phase-pure[20] brookite and anatase/brookite TiO_2 nanostructures were synthesized by hydrothermal method using titanium sulphide as the precursor in NaOH solutions. The phase composition was controlled by the solution concentration and reaction time, and the phase transformation mechanism was elucidated, in that anatase and brookite formed from the direct transformation of sodium titanate. Kandiel *et al.* obtained anatase, brookite nanorods and anatase/brookite mixed phases by the thermal hydrolysis of commercial aqueous solutions of titanium bis(ammonium lactate) dihydroxide in the presence of variable concentrations of urea (0.1–6.0 M) as an *in situ* OH^- source.[21]

Anatase NPs were obtained at the lowest urea concentration (0.1 M); anatase/brookite mixtures were obtained at urea concentrations between 0.5 and 5.0 M, and brookite formed at urea concentration ≥6.0 M, showing that this method allows controlling the phase composition by varying the urea concentration.

Most commercial Ti precursors are toxic, undergoing fast hydrolysis and formation of corrosive by-products: Tomita *et al.*[22] prepared single-phase brookite, rutile, and rutile–anatase NPs from a homemade water-soluble titanium(IV) complex $(NH_4)_6[Ti_4-(C_2H_2O_3)_4(C_2H_3O_3)_2(O_2)_4O_2]_4 \cdot H_2O$, stable in a wide range of pH and *T*. The formation of brookite from this titanium complex has been related to the anion structure (Fig. 3a), which is very similar to the brookite architecture. The structural similarity of the complex anion and the brookite architecture allows the directional synthesis of brookite nanopowders. This method is based on the idea that metastable phases often crystallize first during procedures of chimie douce[22] at low *T*, because in a nucleation-controlled regime their nuclei form at lower supersaturation conditions.

Nonetheless, the structural similarity between the dissolved molecules and the nuclei of the solid phase is fundamental: after phase (*e.g.*, brookite) nucleation, the crystallite growth has a lower activation energy that the nucleation of another phase and, this way, the nucleation of the metastable phases is favoured. Unfortunately, this synthesis requires the preparation of the Ti complex, which could hamper a possible scale-up procedure. Recently, T. Ban *et al.* (Fig. 3b) studied in detail the synthesis of phase-pure brookite from aqueous sols of titanate nanosheets, as brookite precursor(s), prepared with mixtures of Ti-isopropoxide (TIP) and tetramethylammonium hydroxide (TMAOH) by hydrothermal treatment at relatively low *T* (*i.e.* as low as 120 °C).[23]

It was found that the nucleation of brookite crystals occurred in the precipitates, then, the adsorption of titanate nanosheets on brookite particles led the particles to transform into rod-like particles, elongated along the *c*-axis.

The transformation of the adsorbed titanate nanosheets into brookite was driven by the underlying brookite crystals and the resulting particles were single crystal-like brookite particles, though with a rough surface. This phenomenon was markedly affected by the presence of TMAOH, in that other tetralkylammonium hydroxides did not lead to brookite formation.

Dosing the glycine concentration during hydrothermal treatment at 200 °C for 20 h allows obtaining phase-pure brookite, phase-pure anatase, or anatase/brookite mixed phases (containing heterojunctions). In the absence of glycine, pH control (as obtained by using NH_4OH or NaOH) led to the formation of anatase and brookite, respectively, in agreement with the fact that NH_4^+ ions and Na^+ ions favour the formation of anatase and brookite, respectively. The brookite content in anatase/brookite mixed phases decreased by increasing the glycine concentration. The so-obtained TiO_2 samples were tested as photocatalysts towards the photodegradation of Cylindrospermopsin (a natural toxin produced by several fresh water cyanobacteria): interestingly, the absorption edges of the mixed phases were red-shifted in the range of 250–400 nm, but unfortunately, the electron–hole recombination efficiency under UV-Vis light in the mixed phase photocatalysts was much lower than that in single phase TiO_2.[24]

H. Xu and Zhang[25] reported a one-pot facile hydrothermal synthesis of brookite/rutile nanocrystals using $TiCl_4$ as Ti precursor and triethylamine to tune the brookite/rutile ratio. The resulting TiO_2 nanocrystals were tested as photocatalysts in the degradation of rhodamine B under simulated solar light: the sample containing 38% brookite and 62% rutile showed the highest photocatalytic activity, which was six times higher than that of the commercial benchmark, Degussa P25 (P25).

According to H. Lin *et al.* the type of exposed crystalline facets is responsible of the photocatalytic activity of brookite: single-crystalline brookite nanosheets surrounded by four {210}, two {101}, and two {201} facets were obtained at basic pH.[26] These nanosheets were very active towards the degradation of organic contaminants, outperforming P25, by decreasing the recombination rates of photogenerated charge carriers, as reducing and oxidizing species. In contrast, phase-pure brookite nanoflowers and nanospindles with irregular crystalline facets were inactive. The authors suggest that a possible strategy to improve its photocatalytic activity would be, therefore, by tailoring brookite morphology and surface structure.

H. Tran *et al.*[11] produced phase-pure brookite, anatase and rutile by a sol–gel synthesis of an amorphous TiO_2 precursor from TIP followed by hydrothermal treatment in different conditions (Fig. 3c). They compared their photocatalytic activity to that of P25 towards the degradation of three contaminants (*i.e.*, cinnamic acid, ibuprofen and phenol) under simulated solar light. The general activity order was: P25 > anatase ≈ brookite > rutile: remarkably, the activities of the brookite and anatase samples obtained under milder hydrothermal
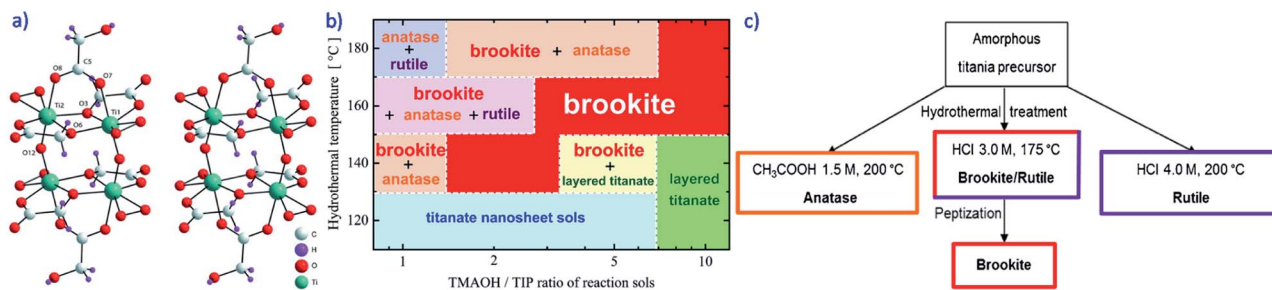
Fig. 3 (a) Stereoview of the anion of the water-soluble complex, synthesised by Tomita *et al.* to get phase-pure brookite.[22] Reproduced with permission from Tomita *et al.* A water-soluble titanium complex for the selective synthesis of nanocrystalline brookite, rutile, and anatase by a hydrothermal method, *Angew. Chem., Int. Ed.*, 2006, John Wiley & Sons Inc. (b) Range of hydrothermal T (110–190 °C) as a function of the TMAOH/TIP ratios that allow obtaining different TiO_2 phases from titanate nanosheets containing sols.[23] Reprinted from *Advanced Powder Technology*, 32, T. Ban, A. Hamajima, N. Akao, C. Takai-Yamashita and Y. Ohya, Hydrothermal synthesis of highly pure brookite-type titanium oxide powder from aqueous salts of titanate nanosheets, 32, 3601–3609, copyright (2021), with permission from Elsevier. (c) Scheme of the sol–gel synthesis of phase-pure TiO_2 polymorphs by hydrothermal treatment of an amorphous TiO_2 precursor obtained by sol–gel method.[11] Reprinted from *Applied Catalysis B: Environmental*, **200**, H. T. T. Tran, H. Kosslick, M. F. Ibad, C. Fischer, U. Bentrup, T. H. Vuong, L. Q. Nguyen and A. Schulz, Photocatalytic Performance of Highly Active Brookite in the Degradation of Hazardous Organic Compounds Compared to Anatase and Rutile, 647–658, copyright (2017), with permission from Elsevier.

conditions (*i.e.*, at $T = 175$–200 °C) were close to that of P25, which is, instead, obtained by pyrolysis in much harsher conditions (*i.e.*, $T > 1800$ °C).

Iskandar *et al.*[27] prepared macroporous brookite particles by spray drying using polystyrene latex particles as colloidal template, followed by calcination at mild T: the fair photocatalytic activity towards the UV degradation of rhodamine B was ascribed to the available macropores, favouring the diffusion of reactants and products.

Besides hydrothermal/solvothermal treatments, the sol–gel method can also be adopted to obtain anatase/brookite mixed phases with photocatalytic properties, *i.e.*, active towards the degradation of water pollutants both under UV[28] and simulated solar light.[29]

Freyria *et al.* studied several undoped TiO_2 NPs obtained by different sol–gel synthesis,[29] either assisted by a soft template or not. It was shown that a template-free method based on pH control, adapted from Mutuma *et al.*,[30] allowed obtaining anatase/brookite and anatase/brookite/rutile mixed phases at acidic pH by calcination at either 200 or 600 °C. The role of brookite was particularly clear with the sample calcined at higher T (600 °C), which was still photocatalytically active under simulated solar light towards the degradation of the emerging pollutant *N*-phenylurea, notwithstanding its lower surface area and the formation of larger rutile-containing particles: as a whole, the so-obtained photocatalysts were able to exploit the (small) UV fraction of solar light, finally competing with commercial P25.

2.2. Perspective role of green synthesis methods

The aforementioned synthesis methods imply several tedious steps, addition of alkalis or acids, high calcination T and a difficult control of multi-phase ratios, leading to materials with low reproducibility, which are not environmentally friendly and energy consuming. Finding greener synthesis methods, based on or assisted by microwaves (MW), ball milling (BM) and

ultra-sound (US)[31] could solve such problems and favour the production of brookite at a larger scale, which could be useful for practical applications.

Hydrothermal methods usually imply long-time reactions (24–72 hours) with T in the 180–250 °C range, resulting time- and energy-consuming methods. To this end, MW-assisted hydrothermal method can shorten the synthesis duration and lower the synthesis T: in the presence of MW, faster kinetics favours the formation of more numerous nuclei and, thus, of smaller NPs. In addition, MW irradiation also affects the phase composition of the obtained TiO_2: in some conditions, MW favour the formation of anatase against rutile, and in other conditions the formation of brookite (along with anatase) is also favoured. This effect on the phase composition is related to the different kinetics under MW irradiation. Other authors obtained higher brookite-content TiO_2 by MW-assisted synthesis, *i.e.*, brookite containing traces of rutile[32] and even phase-pure brookite.[33] As a matter of fact, further studies are required to understand the way the solvent, the precursor and the different phases are affected by MW irradiation.

Other authors found that a synthesis at mild T, based on the use a DES (Deep Eutectic Solvent),[34] allows obtaining brookite/rutile materials with remarkable photocatalytic activity and outperforming P25 in the production of H_2 from water reduction. The photocatalytic activity has been ascribed to the presence of brookite/rutile heterojunctions and defects, as obtained by employing a DES in autoclave at 180 °C for 18 hours, followed by centrifugation, washing and drying at 60 °C, *i.e.* avoiding any calcination procedures. The DES was able to allow the formation of brookite/rutile heterojunctions and lattice dislocations and disorders, which can enhance the light absorption and exposure of more active sites. When the defects were repaired, the photocatalytic activity decreased.

BM can be adopted to favour phase-transitions and, in principle, should be used with the aim of favouring the formation of brookite, since anatase is less stable than brookite

(and rutile, of course). Indeed, by BM of a P25 sample (containing 82% anatase and 18% rutile),[35] a significant transition of anatase to rutile and brookite occurred (the ball milled P25 contained 47% anatase, 24% rutile and 29% brookite) and the band gap decreased from 3.10 eV to 2.97 eV.

BM methods are usually based on trial-and-error procedures, but a systematic analysis could lead to find the optimal conditions to obtain brookite-containing TiO_2. In fact, brookite NPs showed high resistance to shock-waves (300 shocks, 2.0 MPa) without any shift or peak broadening in the XRD patterns, at variance with anatase NPs, which undergo, instead, transition to rutile.[36]

Some earlier works report on the use of US on the synthesis of anatase/brookite phases with interesting photocatalytic properties: for instance, US have been found to favour the formation of brookite during a room T synthesis of nanoporous anatase/brookite photocatalysts outperforming P25 in the degradation of rhodamine B.[37] The mixed phase was well crystallized, with no rutile formation, after US treatment at room temperature, without the need of thermal treatments, which are normally adopted to induce crystallization. Similarly,[38] a mesoporous anatase/brookite mixed phase was obtained by US, allowing the agglomeration of monodispersed TiO_2 particles, in the presence of a surfactant, to obtain mesoporosity and high surface area, both properties positively affecting the activity towards the oxidation of n-pentane with air, during which the US prepared material outperformed P25.

3. Is the brookite band gap really fundamental for its photocatalytic applications?

Notoriously, the photocatalytic activity of TiO_2 strongly depends on its E_g, but also on its phase structure, crystallite size, specific surface area and pore structure; nonetheless, with mixed phases, the presence of heterojunctions is crucial.

Concerning the band gap, based on *ab initio* electronic structure calculations[39] and photoemission spectroscopy,[40] it is generally acknowledged that the valence band (VB) of TiO_2 has an O 2p character, with some Ti 3d hybridization, whereas the conduction band (CB) has a Ti 3d character, with some O 2p hybridization (Fig. 1).

The E_g of brookite deserves some attention:[41] for some time it has been unclear whether brookite was a direct or indirect semiconductor.[6,42] An indirect band gap of 1.9 eV (*i.e.*, in the visible) had been once reported for mineral brookite,[42] confirming the need of shedding some light on this subject, although the fact that mineral samples were considered in ref. 42 may have led to a determination of a value that is not proper of pure brookite. Currently, it is acknowledged that brookite is a direct semiconductor (like rutile), at variance with anatase, which is an indirect semi-conductor.[4,6]

At variance with rutile and anatase, for which the average values reported in the literature are *ca.* 3.0 eV and 3.2 eV, respectively, the reported experimental E_g values for brookite span from 3.1 to 3.4 eV (see Table 1).[41] Besides this, the experimental determination of the optical band gap may be affected by some approximation error, as by the Tauc plot method an assumption is made whether the electronic transition is direct or indirect and, thus, the reported band gap values have to be considered with care, especially with mixed phases. A fair approximation is the determination of the band gap by at least two different methods (by means of the Tauc plot and by extrapolating the onset of absorption, for instance) and then a comparison of the obtained values within the set of studied samples, as remarked by some authors.[29,43]

Nonetheless, some (earlier) theoretical approaches should be considered with care: DFT methods may significantly underestimate the E_g values of semi-conductors, because of many-body quasiparticle effects. Although the experimentally observed tendency for the three polymorphs of TiO_2 agrees with the theoretical ones, with brookite there is still a lack of understanding, which is related to the complexity of the material. All this notwithstanding, from the photocatalytic point of view, determination of the flat band potential, of trap states energy level of defects and impurities is crucial.

A DFT study (under the nonlocal B3LYP approximation)[44] of the structural and electronic properties of the low-index surfaces of brookite allowed calculating surface energies, band energy values, and the response to hydrostatic pressure of the bulk and the surfaces of brookite. All the studied surfaces were considered as direct semi-conductor as well as the bulk. In addition, pressure-induced phase transformations were predicted from the anatase and the rutile polymorph to the brookite polymorph at about 3.8 and 6.2 GPa, respectively. It was found that the orthorhombic structure and the fractional coordinates of brookite vary isotropically with the increase in pressure. The zero-pressure calculated E_g of bulk polymorphs were: 3.24 eV (rutile), 3.59 eV (anatase) and 3.78 eV (brookite). The calculated brookite surface stabilities followed the order (010) < (110) < (100), and the minimum E_g of 2.78 eV value was found for the (110) surface, whereas E_g of 3.69 eV and 4.63 eV were calculated for the (100) and the (010) surfaces. The lower value of the (110) surface was ascribed to the minor stabilization of the Fermi energy showing the flattest VB topology. The pressure was found to affect the band gap value in a different way for the different TiO_2 polymorphs studied. Specifically, the E_g values of rutile and brookite (both direct semi-conductors) increase with pressure, as the CB moves to higher energy due to the shortening of the Ti–O bond and to the higher repulsion between the involved orbitals. Instead, the E_g of anatase, which is an indirect semi-conductor, decreases at higher pressure (Fig. 4a). Buckeridge *et al.*[6] showed that the relative position of anatase and brookite bands can help the e^-/h^+ stabilization. In their paper, they considered eight TiO_2 polymorphs, of which they calculated the ionization potential (I, by using the QM/MM approach), the E_g (by using plane waves DFT), and derived the electron affinity (A) as $A = I - E_g$.

The electronic structure of eight known polymorphs of TiO_2 was examined and their I and A values were aligned relatively to an absolute energy reference (Fig. 4b). Interestingly, it was found that for photocatalytic applications, the anatase/brookite
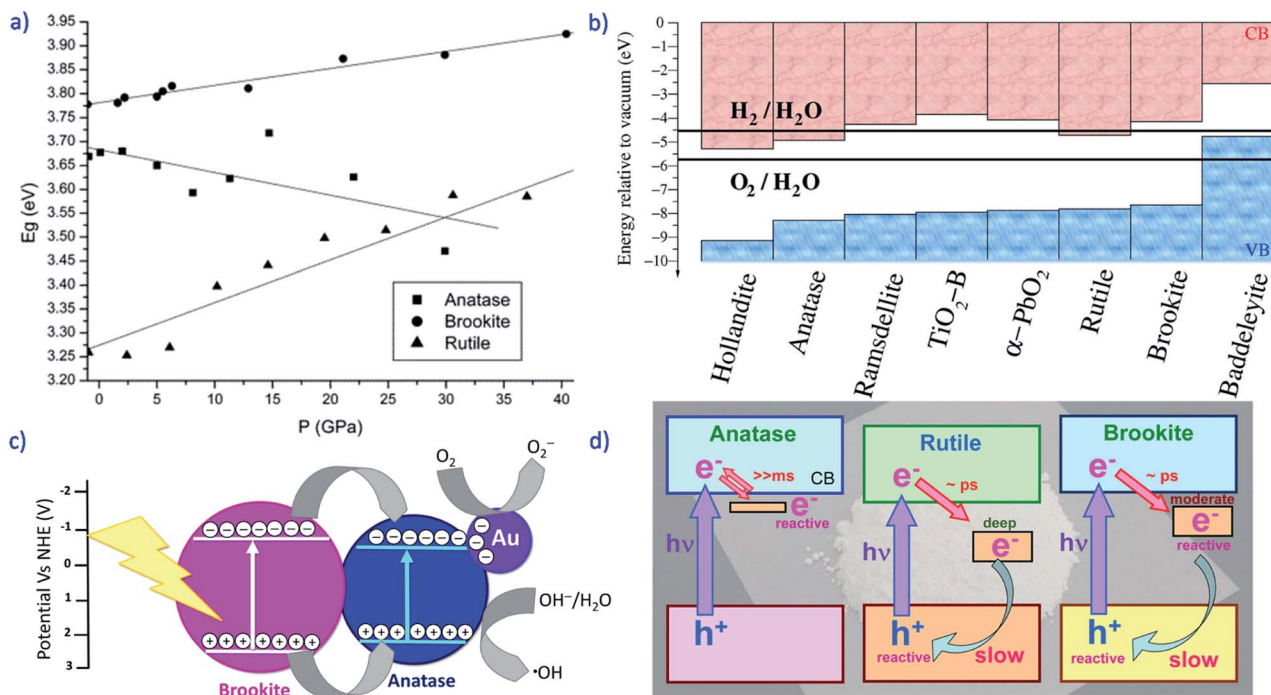
Fig. 4 (a) Effect of pressure on the E_g values (eV) of anatase (squares), rutile (triangles) and brookite (circles).[44] Reprinted with permission from A. Beltrán, L. Gracia and J. Andrés, *Journal of Physical Chemistry B*, 2006, **110**, 23417–23423. Copyright (2006), American Chemical Society. (b) Calculated positions of the valence band (VB) and of the conduction band (CB) (referred to the vacuum level) for the eight polymorphs of TiO$_2$, in comparison to the redox potentials of H$_2$ and O$_2$.[6] Reprinted with permission from J. Buckeridge, K. T. Butler, C. R. A. Catlow, A. J. Logsdail, D. O. Scanlon, S. A. Shevlin, S. M. Woodley, A. A. Sokol and A. Walsh, *Chemistry of Materials*, 2015, **27**, 3844–3851. Copyright (2015), American Chemical Society. (c) Band gap alignment of brookite and anatase (*vs.* normal hydrogen electrode potential) and effect of Au NPs deposited on anatase according to ref. 48. (d) Depth of the electron traps in anatase, rutile and brookite.[49] Reprinted with permission from J. J. M. Vequizo, H. Matsunaga, T. Ishiku, S. Kamimura, T. Ohno and A. Yamakata, *ACS Catalysis*, 2017, **7**, 2644–2651 copyright (2017), American Chemical Society.

pair was an optimal combination of phases to enhance activity in the visible spectrum due to the relative band alignment.

Some of the applications of the so-obtained results were particularly intriguing: a favourable CB position for photo-electrochemical water splitting was found in the brookite phase, in agreement with experimental results showing that thin film samples of brookite outperform anatase and rutile[5,45] According to Buckeridge *et al.*[6] the more favourable band alignment would provide a greater thermodynamic driving force for the reduction half-reaction. Moreover, as for the rutile/anatase pair (occurring in P25), also for the anatase/brookite pair, two factors could contribute to the enhanced performance of the mixture, *i.e.*, the increased efficiency of e$^-$/h$^+$ separation and a reduction in the effective E_g.

As mentioned before, the theoretical calculations reported by Buckeridge *et al.*[6] are confirmed by a series of experimental results: for instance, anatase/brookite mixed-phases have been used for photocatalytic degradation of the methylene blue dye, showing that the mixed-phase outperformed the pure phases.[46] By photoluminescence (PL) measurements, it was found that mixed anatase/brookite mixed phase showed reduced PL in comparison to the pure phases, indicating an increased charge separation.[47] The synergistic effect of anatase/brookite mixed phases has been demonstrated also towards the production of H$_2$ and the degradation of diclophenac under UV irradiation:[13]

Khedr *et al.* obtained phase-pure anatase and brookite and different anatase/brookite mixed phases by hydrothermal methods. The TiO$_2$ crystallites size was smaller in the mixed phases, with respect to phase-pure ones, likely due to the fact that the crystalline growth is limited when two phases form simultaneously.

The absorption edge of the mixed phases slightly shifted towards the visible range, likely due to the interparticle charge from the VB of one phase to the CB of the other phase, as a consequence of type II heterojunctions.

Finally, PL measurements showed also in this case that the charge carriers had longer lifetime with mixed phases, indicating a more efficient separation of charges. The photocatalytic activity[20] of anatase/brookite TiO$_2$, phase-pure anatase NPs and phase-pure brookite nanoplates was studied towards the reaction of H$_2$ evolution in aqueous methanol solution.

The anatase/brookite TiO$_2$ and brookite nanoplates were more active as compared to phase-pure anatase NPs, despite a lower surface areas area of the mixed phases. Based on Mott–Schottky analysis, brookite nanoplates have a more cathodic CB edge potential than anatase, leading to more energetically favourable hydrogen reduction. Femtosecond transient absorption spectroscopy (TAS) measurements suggest that the photoexcited electrons transfer from brookite to anatase phase, leading to further enhancement of the photocatalytic activity. In

comparison with the commercial benchmark photocatalyst (*i.e.*, highly active P25), the anatase/brookite TiO$_2$ was 220% more active when the H$_2$ yield per unit area of the photocatalyst surface was considered.

The UV photocatalytic activity of anatase NPs, of anatase/brookite mixtures, and of brookite nanorods was assessed by H$_{2(g)}$ evolution from aqueous methanol solution and by the degradation of dichloroacetic acid (DCA).[21] Interestingly, a higher H$_2$ evolution activity was measured with anatase/brookite mixtures and brookite, notwithstanding the lower surface area with respect to anatase NPs. Such a result was explained by considering that, with brookite nanorods, larger secondary particles formed, but also that the larger crystallites size of brookite in nanorods with fewer defects should be regarded as another explanation. The flat band potential and the quasi-Fermi level of the anatase NPs and the brookite nanorods CB were determined: both values were shifted more cathodically with brookite nanorods, the magnitude of the shift agreeing with the difference in the measured E_g values (E_g = 3.18 eV and E_g = 3.31 eV for anatase and brookite, respectively). On the contrary, in case of the photocatalytic degradation of DCA, anatase/brookite mixtures and phase-pure brookite exhibit lower photocatalytic activity than phase-pure anatase NPs. This behaviour well correlates with the surface area of the investigated powders.

The positive effect of anatase/brookite heterojunctions has been shown also with anatase/brookite nanowires on which Au NPs were deposited and tested for the photocatalytic removal of resorcinol under UVA irradiation (Fig. 4c).[48] In the proposed scheme, the photogenerated electrons move from brookite to anatase, accelerating the charge carriers separation. The brookite CB minimum and VB maximum values were −0.7 V and +2.6 V, respectively, with an E_g value of 3.3 eV. The anatase CB minimum and VB maximum values were −0.5 V and +2.7 V, respectively, with an E_g value of 3.2 eV. In addition, the supported Au NPs acted as an antenna, further prohibiting the recombination of charge carriers (Fig. 4c).

Vequizo *et al.*[49] used femtosecond to millisecond time-resolved visible to mid-IR absorption spectroscopy to study the behaviour of photogenerated e⁻/h⁺ in anatase, rutile and brookite.

Interestingly, most of the photogenerated e⁻ in brookite are trapped at powder defects within a few picoseconds: this phenomenon, though decreasing the number of free electrons, extends the lifetime of both holes and trapped electrons, thanks to the (optimal) depth of the electron trap (*ca.* 0.4 eV) in brookite (Fig. 4d). Consequently, the number of surviving holes, available for photocatalytic oxidation, increases; simultaneously, trapping decreases the reactivity of electrons to some extent, but they remain active for photocatalytic reduction processes. The same phenomenon (electron trapping) also takes place on anatase and rutile powders, but the trap-depth in anatase is too shallow (*ca.* 0.1 eV) to extend the lifetime of holes, whereas in rutile is too deep (*ca.* 0.9 eV) for photocatalytic reduction reactions.

When the electron-trap depth is comparable to the thermal energy at room T ($kT \sim 0.03$ eV), like in anatase, free electrons

and trapped electrons are thermally equilibrated, and are hardly distinguishable. The reported results indicate that the electron traps in different TiO$_2$ powders grow deeper in the order: rutile > brookite > anatase.

The different depth of the electron-trap comes from the difference in the "softness" of the defects that trap the electrons. The origin of the electron trap is a defect such as an oxygen vacancy or interstitial Ti-site.[50,51] The Ti^{4+} species around the defects capture electrons to form Ti^{3+} with structural deformation. The depth of the electron trap depends on how the defects stabilize the trapped electrons through structural relaxation (formation of polaron, *i.e.*, a quasi-particle consisting of a charge carrier associated to a lattice deformation): as the lattice of a particle becomes more deformed, the trapped electrons become increasingly stabilized. Theoretical calculations predicted stabilization energies of 0.8–1 eV and 0–0.2 eV for rutile and anatase, respectively.[50,51] Such "moderate and appropriate depth" of the electron trap in brookite powders of different origin, particle morphology and size, makes both electrons and holes reactive for photocatalytic reactions.

The efficient transport of electrons and holes through the material is crucial for many of its photochemical and photoelectrochemical applications. In TiO$_2$, there is a strong electron/photon coupling, and thus photogenerated electrons and holes can self-trap, forming small polarons.

Carey *et al.*[52] adopted a hybrid DFT approach to predict the mobility of holes in anatase, brookite, and TiO$_2$–B, *i.e.*, the three phases of TiO$_2$ where hole polarons are predicted to be stable. They found that brookite is characterized by the highest hole mobility, which increases in the order TiO$_2$–B < anatase < brookite. Moreover, there are also differences in the character of holes migration, which implies the thermal ionization of small polarons followed by long-range band-like diffusion and subsequent re-trapping in brookite, whereas for the other two polymorphs studied, holes migration has a mixed character.

4. A sneak peek into some brookite properties: brookite is the new black (TiO$_2$) and favours the transport of Li$^+$ ions

Since its discovery and first synthesis in harsh conditions (*i.e.* by hydrogenation at p_{H_2} = 20 bar at 200 °C for five days[53]), black TiO$_2$ has attracted a lot of attention due to its effective absorption of both the IR and the vis range.[54] TiO$_2$ reduction is usually attained by harsh methods, like plasma treatment, vacuum activation at high T, electron beams irradiation,[55] reduction with molten Al,[56] which acts as a reductant in a two-zone vacuum furnace, lowering oxygen partial pressure at different T (300–600 °C).

One of the drawbacks of black TiO$_2$ is, however, its poor stability to moisture/air: Zhu *et al.*[56] showed that considerable amounts of Ti^{3+} states and oxygen vacancies are introduced into brookite platelets, inducing, simultaneously, a unique crystalline core/disordered shell structure of the type TiO$_2$@TiO$_{2−x}$. In this case, the so-obtained black brookite in contact with air for

a long time maintained high photocatalytic activity for solar and vis photocatalytic degradation of the organic pollutant methyl orange. In our opinion, this result is particularly interesting, as it could be ascribed to a specific ability of brookite to stabilize defects within its crystalline structure, having tunnels across the c axis, which are also able to favour the transport of Li^+ ions, *vide infra*.[8]

Besides the removal of aqueous pollutants, the main interest for black TiO_2 derives from its use in reactions of environmental interests, like the reduction of CO_2 for which TiO_2 is still a promising photocatalyst due to the favourable band edges, since the CB edge of TiO_2 is higher than the potential of CO_2 reduction. Indeed, black brookite single-crystalline nanosheets showed outstanding photocatalytic activity towards the reduction of CO_2 under solar light.[57] The black TiO_2 was, however, prepared by a multi-step procedure, starting from oxidation of commercial TiH_2 by H_2O_2, followed by reduction with $NaBH_4$, HCl treatment and under vacuum treatment at increasing T (up to 700 °C). Interestingly, no phase transition to anatase/rutile occurred, the so-obtained brookite being stable up to 700 °C. The reported physico-chemical characterization showed that by following this preparation technique, Ti^{3+} sites were mainly located in the bulk.

Concerning the aforementioned transport/storage of Li^+ ions, Yoon *et al.*[32] found that the discharge capacity of brookite obtained by MW-assisted method was lower than that of rutile and anatase. The capacities of the brookite and anatase TiO_2 phases are related to insertion of lithium into the channels caused by the TiO_6^{2-} octahedral units arrangement along the [001] and [010] directions, respectively, in the brookite and anatase phases. Though it has been reported that the lithium insertion properties of anatase are generally much better than those of brookite, the size and morphology of the TiO_2 polymorphs are also important controlling factors and, thus, there is room for improving the nanometric properties of brookite-containing materials also for the study of Li-insertion capacity for lithium-ion batteries.

5. Surface properties of brookite and the relevance of surface geometry

Sizeable and controllable content of Ti^{3+} species were implanted in phase-pure brookite nanosheets enclosed by {101}, {201}, and {210} facets by hydrothermal method.[10] By properly studying the synthesis conditions, the optimal time of hydrothermal treatment (12 hours) allowed having a high Ti^{3+} defects concentration (54.3%). Such defects were (reactive) Ti^{3+} species, able to positively affect the selectivity of Ru NPs-doped brookite nanosheets in the benzene semi-hydrogenation reaction. The enhanced selectivity to cyclohexene was ascribed to the suppression of cyclohexene molecules adsorption by such Ti^{3+} defects. By increasing the duration of the hydrothermal time from 1 to 12 hours, the content of brookite increased, resulting in the increase of the exposed degree of {210}, {101}, and {201} crystalline facets, and hence, the content of Ti^{3+} defects increased. Brookite has high energy {210}, {101}, and {201} crystalline facets containing many coordinatively-unsaturated

(cus) titanium ions as shown in Fig. 5a, besides a small amount of (saturated) six-fold (Ti6c) atoms, many four-coordinated Ti (Ti4c) and five-coordinated Ti (Ti5c) cus atoms occur at the surface of brookite {101} and {201} facets. Specifically, all the Ti atoms at the {210} facets are cus Ti5c. Such a high proportion of cus Ti atoms on these facets should contribute to the appearance of Ti^{3+} defects. Therefore, the above order of Ti^{3+} content can be rationalized by the evolution of the exposed degree of these facets.

Brookite nanorods with controlled exposed crystalline facets with different aspect ratio (AR ~ 1.6–5.2) were prepared by hydrothermal process with or without polyvinyl alcohol (PVA) or polyvinyl pyrrolidone (PVP) as aspect-controlling agents.[58] Transmission Electron Microscopy and Selected Area Electron Diffraction showed that the brookite nanorods had larger {210} and smaller {212} exposed crystal faces. The photocatalytic activity for the decomposition of toluene under UV irradiation (with a LED emitting at 365 nm for 8 hours) was found to depend on the aspect ratio of the nanorods. Specifically, it increased with an increase in aspect ratio, due to an optimal ratio between the surface area of the {210} and the {212} exposed crystal faces. Oxidation reaction predominantly proceeded on the {212} facet, while the {210} facet was assigned to a reduction site, resulting in the achievement of an effective charge separation and an improvement of photocatalytic activity.

In a second set of experiments (Fig. 5b), Fe ions were selectively adsorbed on the {212}[58] exposed crystal facets and on a commercial brookite (from Kojundo Chemical Laboratory Co, Ltd): during the degradation of acetaldehyde under vis light irradiation (with a LED emitting at 455 nm for 24 hours) the site-selective Fe^{3+}-modified brookite nanorods showed much higher photocatalytic activity than the Fe-loaded commercial brookite TiO_2. Such a behaviour was assigned to an effective separation of the oxidation and reduction processes: oxidation proceed over Fe^{3+} ion-modified {212} faces and reduction on {210} faces of the TiO_2 surface.

The role of different exposed crystalline faces of brookite has been noticed by several authors, who enlightened different aspects. For instance, M. Rodriguez *et al.* made first-principle calculations study of the interaction of CO_2 with the (210) surface of brookite[59] by considering cluster and periodic slab systems and comparing it with the interaction of CO_2 with the (101) anatase surface. On the one side, it was found that the (210) brookite surface had a negligible charge transfer to CO_2 molecules, indicating that unmodified brookite is not a suitable catalyst for CO_2 reduction. On the other side, the modified surface, upon creation of oxygen vacancies may lead to an enhanced CO_2 reduction activity. The theoretical results were corroborated by experimental data concerning the interaction of CO_2 with oxygen-deficient brookite and defect-free brookite: indeed, IR spectroscopy showed the occurrence of the CO_2^- ion when CO_2 was dosed on oxygen-deficient brookite.

Koelsch[60] *et al.* measured the electrochemical properties of sol–gel synthesised anatase and brookite by cyclic voltammetry in water and acetone. The fraction of Ti^{4+} sites able to undergo reduction to Ti^{3+} sites did not differ much in the two phases, but additional signals, observed in the brookite voltammograms,
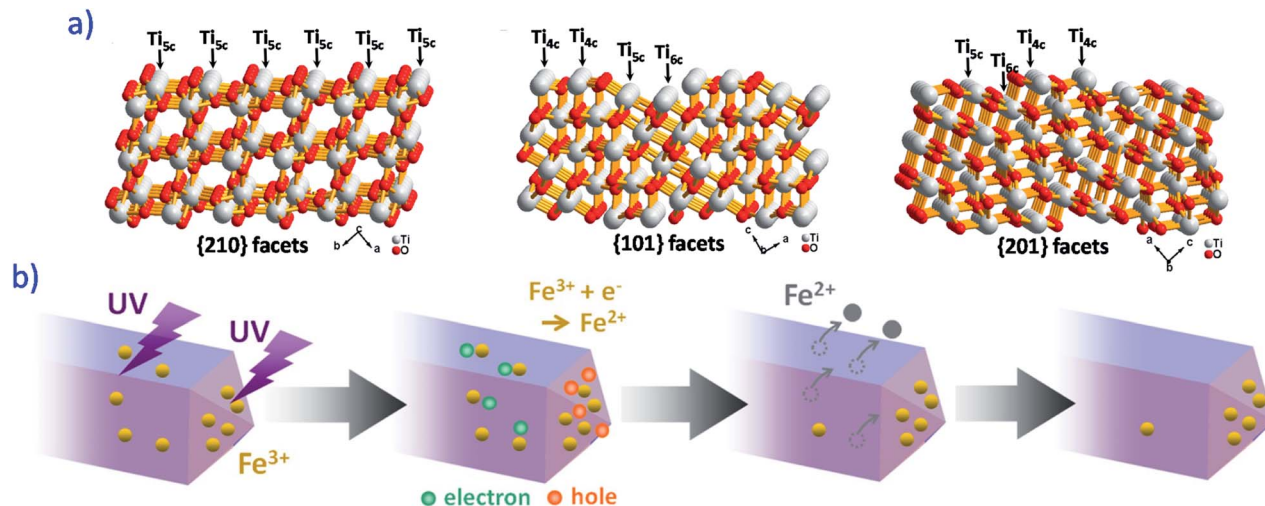
Fig. 5 (a) Atomic structure of brookite TiO_2 {210} (A), {101} (B), and {201} (C) facets.[10] Reprinted from *Journal of Catalysis*, **398**, G. Zhou, F. Wang and R. Shi, Nanoparticulate Ru on morphology-manipulated and Ti^{3+} defect-riched TiO_2 nanosheets for benzene semi-hydrogenation, 148–160, copyright (2021), with permission from Elsevier. (b) Scheme of Fe^{3+} ions expected to mainly adsorb on the {212} faces under UV irradiation.[58] Reprinted from *Journal of Molecular Catalysis A: Chemical*, **396**, T. Ohno, T. Higo, H. Saito, S. Yuajn, Z. Jin, Y. Yang and T. Tsubota, Dependence of photocatalytic activity on aspect ratio of a brookite TiO_2 nanorod and drastic improvement in visible light responsibility of a brookite TiO_2 nanorod by site-selective modification of Fe^{3+} on exposed faces, 261–267, copyright (2015) with permission from Elsevier.

were explained according to a greater electrochemical reactivity of brookite, in that the type of surface states (rather than the concentration of surface defects) were responsible for the different electrochemical response of brookite.

Fufachev[61] *et al.* have shown that the surface of brookite have some peculiar properties, which determine its reactivity towards the ketonization reaction in the gas phase, where brookite is more reactive than anatase, but less than rutile.[61] The superior activity of brookite (with respect to anatase) was ascribed to the surface geometry, and specifically to the Ti–Ti distance (2.96 or 2.99 Å in rutile, 3.56 Å in brookite and in the 3.71–3.83 Å range in anatase), being the shorter distance(s) responsible of the facile formation of bidentate carboxylates at the surface of both rutile and brookite, whereas the formation of monodentate carboxylates was favoured at the surface of anatase. In the studied reaction, the role of the Ti–Ti distance was more pronounced than that of surface acidity, as no clear correlation was found with the surface acidity, which follows the order brookite > rutile > anatase according to pyridine adsorption followed by IR spectroscopy and temperature programmed desorption of ammonia. Specifically, two families of Lewis acidic sites were identified with the three studied polymorphs, namely weaker ones (NH_3 desorption peak of about 200 °C) and stronger ones (NH_3 desorption peak at about 350 °C). Pyridine adsorption confirmed the mainly Lewis nature of acidity: no Bronsted–Lowry sites were detected with anatase and rutile, whereas (few) acidic –OH groups were observed at the surface of brookite.

6. The crucial role of brookite in TiO_2 mixed phases: facts and mysteries

Brookite has a prominent role as a promoter in the anatase-to-rutile (ATR) transition: the presence of brookite in mixed phases favours the ATR transition in different ways. According to Zhang and Banfield,[17,18] anatase is more thermodynamically stable when the NPs diameter is $d < 11$ nm, rutile is more stable when $d > 35$ nm and brookite is more stable when 11 nm $< d <$ 35 nm. Therefore, brookite would transform directly to rutile, whereas anatase could either transform directly to rutile or to brookite and then, to rutile.

Concerning the rate of the transition, the brookite to rutile one should be faster than that of anatase to rutile, therefore the ATR transition should be accelerated by the brookite-to-rutile transition.

Pressure has a non-negligible effect of the ATR transition: it has been reported that the number of potential nucleation sites is the rate-limiting factor in the ATR transition.[62] The pressure of brookite on small anatase crystallites may also accelerate the ATR transition, by reducing the strain energy deriving from the formation of rutile nuclei. The pressure due to brookite attachments to anatase may therefore enhance the ATR transition. Moreover, the presence of brookite/anatase interfaces with high interfacial energy could provide potential nucleation sites for the ATR transition.

Zhang *et al.*[63] reported a general and tuneable method for the synthesis of transition-metal (M) doped brookite nanorods with different dopants (M = V, Cr, Mn, Fe, Co, Ni, Cu, Mo, *etc.*) and different concentrations. The nanorods can selectively expose the {210} surface facets, induced by their strong affinity for an oleylamine, used as stabilizer. This structure is preserved with variable dopant compositions and concentrations, leading to a series of TiO_2 nanorods where single-atom dopants are homogeneously distributed in a brookite-phase solid lattice. Fe doping was particularly interesting, in that Fe can lead to a substantial catalytic activity enhancement for the photocatalytic H_2 production, probably due to a dopant-induced optical absorption improvement.

7. Conclusions and future directions to make brookite great

The open and not-so-dense structure of brookite (more disordered than the anatase and rutile structures) with TiO_6^{2-} octahedra with 6 Ti–O bonds having different lengths could help the stabilization of (defective) Ti^{3+} and oxygen vacancies, not only at the surface, but also in the bulk of the material.

The possibility to tune the type of exposed crystalline facets could be exploited in relevant photo- and electrochemical processes (*i.e.*, CO_2 reduction and H_2 production), as it may allow a tailored stabilization of the photogenerated electrons/holes.

However, this aspect so far has been less explored: as compared to anatase, tuning the crystal shape and phase has been more difficult with brookite, but there is room for exploring synthesis procedures allowing the preferential exposure of some specific crystalline facets. Brookite exposes mainly the (210) facets with five- and six-coordinated Ti ions (Ti5c and Ti6c), which are more distorted with respect to the sites in anatase and could be more reactive: this could have an effect also of metal/brookite interactions and an impact on heterogeneous catalysis.

Besides trying to elucidate the role of brookite in anatase/brookite and rutile/brookite heterojunctions, which could expand its use in both photo- and photo-electrocatalytic processes, it would be crucial to find greener synthesis methods of brookite and brookite-containing TiO_2 allowing a facile scale-up to produce these NMs in sizeable amounts. From this point of view, while microwaves seem to favour the formation of anatase, as they favour fast nucleation and, thus, anatase is stable as small NPs, ball milling may favour the formation of brookite (over anatase) and ultrasound may favour the formation of anatase/brookite phases avoiding high T treatments. For these reasons, there is room for improving green synthesis methods or other technologies, like laser ablation in air,[64] to control and tailor the synthesis of brookite and brookite-containing mixed phase.

Conflicts of interest

There are no conflicts to declare.

Acknowledgements

Notes and references

1 W. Zhao, Y. Li and W. Shen, *Chem. Commun.*, 2021, **57**, 6838–6850.

2 T. Zhu and S. P. Gao, *J. Phys. Chem. C*, 2014, **118**, 11385–11396.

3 D. Hanaor, C. Sorrell, D. A. H. Hanaor and C. C. Sorrell, *J. Mater. Sci.*, 2011, **46**, 855–874.

4 J. Zhang, P. Zhou, J. Liu and J. Yu, *Phys. Chem. Chem. Phys.*, 2014, **16**, 20382–20386.

5 A. di Paola, M. Bellardita and L. Palmisano, *Catalysts*, 2013, **3**, 36–73.

6 J. Buckeridge, K. T. Butler, C. R. A. Catlow, A. J. Logsdail, D. O. Scanlon, S. A. Shevlin, S. M. Woodley, A. A. Sokol and A. Walsh, *Chem. Mater.*, 2015, **27**, 3844–3851.

7 M. Posternak, A. Baldereschi, E. J. Walter and H. Krakauer, *Phys. Rev. B: Condens. Matter Mater. Phys.*, 2006, **74**, 1–8.

8 D. Dambournet, I. Belharouak, J. Ma and K. Amine, *J. Mater. Chem.*, 2011, **21**, 3085–3090.

9 H. Lin, L. Li, X. Huang, X. Chen, G. Li and R. Yu, *J. Am. Chem. Soc.*, 2012, **134**, 8328–8833.

10 G. Zhou, F. Wang and R. Shi, *J. Catal.*, 2021, **398**, 148–160.

11 H. T. T. Tran, H. Kosslick, M. F. Ibad, C. Fischer, U. Bentrup, T. H. Vuong, L. Q. Nguyen and A. Schulz, *Appl. Catal., B*, 2017, **200**, 647–658.

12 M. Hezam, S. M. H. Qaid, I. M. Bedja, F. Alharbi, M. K. Nazeeruddin and A. Aldwayyan, *Crystals*, 2019, **9**, 1–8.

13 T. M. Khedr, S. M. El-Sheikh, E. Kowalska and H. M. Abdeldayem, *J. Environ. Chem. Eng.*, 2021, **9**, 106566.

14 T. Balaganapathi, B. KaniAmuthan, S. Vinoth and P. Thilakan, *Mater. Res. Bull.*, 2017, **91**, 114–121.

15 D. Reyes-Coronado, G. Rodríguez-Gattorno, M. E. Espinosa-Pesqueira, C. Cab, R. de Coss and G. Oskam, *Nanotechnology*, 2008, **19**, 145605.

16 Y. Wang, Y. Zou, Q. Shang, X. Tan, T. Yu, X. Huang, W. Shi, Y. Xie, G. Yan and X. Wang, *Trans. Tianjin Univ.*, 2018, **24**, 326–339.

17 H. Zhang and J. F. Banfield, *J. Phys. Chem. B*, 2000, **104**, 3481–3487.

18 H. Zhang and J. F. Banfield, *J. Mater. Chem.*, 1998, **8**, 2073–2076.

19 Y. Hu, H. L. Tsai and C. L. Huang, *J. Eur. Ceram. Soc.*, 2003, **23**, 691–696.

20 Q. Tay, X. Liu, Y. Tang, Z. Jiang, T. C. Sum and Z. Chen, *J. Phys. Chem. C*, 2013, **117**, 14973–14982.

21 T. A. Kandiel, A. Feldhoff, L. Robben, R. Dillert and D. W. Bahnemann, *Chem. Mater.*, 2010, **22**, 2050–2060.

22 K. Tomita, V. Petrykin, M. Kobayashi, M. Shiro, M. Yoshimura and M. Kakihana, *Angew. Chem., Int. Ed.*, 2006, **45**, 2378–2381.

23 T. Ban, A. Hamajima, N. Akao, C. Takai-Yamashita and Y. Ohya, *Adv. Powder Technol.*, 2021, **32**, 3601–3609.

24 S. M. El-sheikh, T. M. Khedr, G. Zhang, V. Vogiazi, A. A. Ismail, K. O. Shea and D. D. Dionysiou, *Chem. Eng. J.*, 2017, **310**, 428–436.

25 H. Xu and L. Zhang, *J. Phys. Chem. C*, 2009, **113**, 1785–1790.

26 H. Lin, L. Li, M. Zhao, X. Huang, X. Chen, G. Li and R. Yu, *J. Am. Chem. Soc.*, 2012, **134**, 8328–8331.

27 F. Iskandar, A. B. D. Nandiyanto, K. M. Yun, C. J. Hogan, K. Okuyama and P. Biswas, *Adv. Mater.*, 2007, **19**, 1408–1412.

28 P. Singla, A. Gupta, K. Singh and O. P. Pandey, *Ceram. Int.*, 2021, **47**, 30702–30710.

29 F. S. Freyria, N. Blangetti, S. Esposito, R. Nasi, M. Armandi, V. Annelio and B. Bonelli, *ChemistryOpen*, 2020, **9**, 903–912.

30 B. K. Mutuma, G. N. Shao, W. Duck and H. Taik, *J. Colloid Interface Sci.*, 2015, **442**, 1–7.

31 M. Manzoli and B. Bonelli, *Catalysts*, 2018, **7**, 262.

32 S. Yoon, E. S. Lee and A. Manthiram, *Inorg. Chem.*, 2012, **51**, 3505–3512.

33 Y. Morishima, M. Kobayashi, V. Petrykin, M. Kakihana and K. Tomita, *J. Ceram. Soc. Jpn.*, 2007, **115**, 826–830.

34 Q. Wang, H. Ren, Y. Zhao, X. Xia, F. Huang, G. Cui, B. Dong and B. Tang, *J. Mater. Chem. A*, 2019, **7**, 14613–14619.

35 N. G. Kostova, M. Fabián, J. Briančin, M. Baláž, J. Ficeriová and A. Eliyas, *Bull. Mater. Sci.*, 2021, **44**, 228.

36 A. Sivakumar, S. Kalaiarasi, S. S. J. Dhas, A. I. Almansour, R. S. Kumar, N. Arumugam and S. A. M. B. Dhas, *J. Mater. Sci.: Mater. Electron.*, 2021, **32**, 15134–15142.

37 H. U. Lee, S. C. Lee, J. H. Seo, W. G. Hong, H. Kim, H. J. Yun, H. J. Kim and J. Lee, *Chem. Eng. J.*, 2013, **223**, 209–215.

38 J. C. Yu, L. Zhang and J. Yu, *Chem. Mater.*, 2002, **14**, 4647–4653.

39 F. de Angelis, C. di Valentin, S. Fantacci, A. Vittadini and A. Selloni, *Chem. Rev.*, 2014, **114**, 9708–9753.

40 R. G. Egdell, S. Eriksen and W. R. Flavellt, *Oxygen Deficient SnO₂ (110) And TiO₂ (110): A Comparative Study By Photoemission*, 1986, vol. 60.

41 M. Monai, T. Montini and P. Fornasiero, *Catalysts*, 2017, **7**, 304.

42 R. Zallen and M. P. Moret, *Solid State Commun.*, 2006, **137**, 154–157.

43 R. López and R. Gómez, *J. Sol-Gel Sci. Technol.*, 2012, **61**, 1–7.

44 A. Beltrán, L. Gracia and J. Andrés, *J. Phys. Chem. B*, 2006, **110**, 23417–23423.

45 H. Pan, X. Qiu, I. N. Ivanov, H. M. Meyer, W. Wang, W. Zhu, M. P. Paranthaman, Z. Zhang, G. Eres and B. Gu, *Appl. Catal., B*, 2009, **93**, 90–95.

46 Y. Jiao, F. Chen, B. Zhao, H. Yang and J. Zhang, *Colloids Surf., A*, 2012, **402**, 66–71.

47 H. U. Lee, Y. C. Lee, S. C. Lee, S. Y. Park, B. Son, J. W. Lee, C. H. Lim, C. J. Choi, M. H. Choi, S. Y. Lee, Y. K. Oh and J. Lee, *Chem. Eng. J.*, 2014, **254**, 268–275.

48 L. A. Al-Hajji, A. A. Ismail, A. Bumajdad, M. Alsaidi, S. A. Ahmed, F. Almutawa and A. Al-Hazza, *J. Mater. Sci.: Mater. Electron.*, 2021, **32**, 19764–19777.

49 J. J. M. Vequizo, H. Matsunaga, T. Ishiku, S. Kamimura, T. Ohno and A. Yamakata, *ACS Catal.*, 2017, **7**, 2644–2651.

50 G. Mattioli, F. Filippone, P. Alippi and A. Amore Bonapasta, *Phys. Rev. B: Condens. Matter Mater. Phys.*, 2008, **74**, 241201.

51 S. Na-Phattalung, M. F. Smith, K. Kim, M. H. Du, S. H. Wei, S. B. Zhang and S. Limpijumnong, *Phys. Rev. B: Condens. Matter Mater. Phys.*, 2006, **73**, 125205.

52 J. J. Carey, J. A. Quirk and K. P. McKenna, *J. Phys. Chem. C*, 2021, **125**, 12441–12450.

53 X. Chen, L. Liu, I. Yu Peter and S. S. Mao, *Science*, 2011, **331**, 746–750.

54 X. Liu, G. Zhu, X. Wang, X. Yuan, T. Lin and F. Huang, *Adv. Energy Mater.*, 2016, **6**, 1600452.

55 S. G. Ullattil, S. B. Narendranath, S. C. Pillai and P. Periyat, *Chem. Eng. J.*, 2018, **343**, 708–736.

56 G. Zhu, T. Lin, X. Lü, W. Zhao, C. Yang, Z. Wang, H. Yin, Z. Liu, F. Huang and J. Lin, *J. Mater. Chem. A*, 2013, **1**, 9650–9653.

57 X. Xin, T. Xu, L. Wang and C. Wang, *Sci. Rep.*, 2016, **6**, 23684.

58 T. Ohno, T. Higo, H. Saito, S. Yuajn, Z. Jin, Y. Yang and T. Tsubota, *J. Mol. Catal. A: Chem.*, 2015, **396**, 261–267.

59 M. M. Rodriguez, X. Peng, L. Liu, Y. Li and J. M. Andino, *J. Phys. Chem. C*, 2012, **116**, 19755–19764.

60 M. Koelsch, S. Cassaignon, J. F. Guillemoles and J. P. Jolivet, *Thin Solid Films*, 2002, **404**, 312–319.

61 E. v. Fufachev, B. M. Weckhuysen and P. C. A. Bruijnincx, *ChemSusChem*, 2021, **14**, 2710–2720.

62 A. A. Gribb and J. F. Banfield, *Particle size effects on transformation kinetics and phase stability in nanocrystalline TiO₂*, 1997, vol. 82.

63 Z. Zhang, Q. Wu, G. Johnson, Y. Ye, X. Li, N. Li, M. Cui, J. D. Lee, C. Liu, S. Zhao, S. Li, A. Orlov, C. B. Murray, X. Zhang, T. B. Gunnoe, D. Su and S. Zhang, *J. Am. Chem. Soc.*, 2019, **141**, 16548–16552.

64 Z. Lin, S. Shen, Z. Wang and W. Zong, *iScience*, 2021, **24**, 102469.